

The effect of Cu dopant on structural and optical properties of spray deposited CdS films

تأثير تركيز النحاس على الخواص التركيبية والبصرية لأغشية المركب cds

M. A. Al-Hur

Department of Physics, College of Science, University of Karbala

Abstract

CdS and copper doped $Cd_{1-x}SCu_x$ thin films have been prepared by the spray pyrolysis method. The optical band gaps of pure and doped CdS were found to be varied from 2.34 to 2.45 eV with increase x from 0 to 0.1. The X-ray diffraction (XRD) analysis revealed that the films were polycrystalline and exhibited two phases cubic and hexagonal structure with increasing the hexagonal phase with increasing Cu ratio.

Keywords: CdS, spray pyrolysis, optical properties, Cu concentration.

الخلاصة

تم تحضير أغشية رقيقة للمركب CdS بعد تطعيمه بنسب مختلفة من النحاس (x=0,0.05. 0.1) . فجوة الطاقة البصرية للمركب CdS في الحالة النقية و المطعمة كانت تتغير من (2.34-2.42eV) مع زيادة تركيز المحتوى x كذلك الحال في بقية الثوابت البصرية التي تم حسابها، حيث بينت نتائج تحليل الاشعة السينية (XRD) أن الأغشية المحضرة متعددة التبلور وذات طورين من التركيب (المكعب السداسي) وزيادة الطور السداسي مع زيادة تركيز نسب النحاس المضاف.

Introduction

CdS films are widely used as a window layer in heterojunction solar cells owing to their wide band gap and the ease with which the material can be prepared by low cost methods. CdS has direct band gap of 2.4 eV, which falls in the visible spectrum at room temperature^[1]. CdS can exist in two phases, hexagonal with $a=4.1370 \text{ \AA}$ and $c=6.7144 \text{ \AA}$ ^[2] and cubic with $a=5.8330 \text{ \AA}$ ^[3], the hexagonal (wurtzite) CdS films are preferable for solar cell applications due to their excellent stability in photoelectric conversion and heterogeneous photo catalysis. However, it is not easy to obtain the film having a hexagonal structure only^[4].

Experimental Procedure

Prior to deposit films, the glass substrates were cleaned in with cleaner solution, distilled water and followed by alcohol using ultrasonic bath.

$Cd_{1-x}SCu_x$ films were prepared by using an aqueous solution which contained $CdCl_2$, $CuCl_2$ and thiourea. In the solution, the Cd +Cu to S ratio was maintained at 1:1.5. The excess sulfur was used to maintain stoichiometry in the films. The high substrate temperature causes loss of sulfur during deposition. The cadmium concentration in the solution was (1-x)*1M. The Cu concentration in the solution was (x)*1M (where x=0, 0.05 and 0.10). The ionic solution was sprayed onto hot glass substrates held at 673K using compressed air as the carrier gas. The spray rate employed was 3 mL per min.

X-ray diffraction (XRD) pattern of the CdS film deposited on corning glass substrate is recorded by SHIMADZU XRD-6000 X-ray diffractometer ($CuK\alpha$ radiation $\lambda=0.154nm$) in 2θ range from 20° to 60° . The interplaner distanced d_{hkl} for different planes is measured using Bragg law^[5]

$$2d \sin \theta = m \lambda \quad \dots\dots\dots 1$$

Where d is the interference distance, θ is Bragg's angle , m is order level and λ is the incident wave length

While the average crystallite size (b) estimated by Scherrer's formula [6]:

$$b = \frac{0.89 \lambda}{\Delta(2\theta) \cdot \cos(\theta)} \dots\dots\dots 2$$

Where Δ is half width maximum.

The thickness of prepared films was about 500 nm which measured by Michelson interferometer. An optical transmittance and absorbance spectra were recorded, at room temperature, in the wavelength range (400-1100nm) using OPTIMA SP-3000 UV-Vis spectrophotometer.

The absorption coefficient (α) of pure and Cu-doped CdS thin films were calculated from the optical transmittance spectrum measurements using the formula^[7]:

$$\alpha = \frac{1}{t} \ln \left(\frac{1}{T} \right) \dots\dots\dots 3$$

where t is the thickness of thin films, and T is the transmittance intensity. The energy gap and optical constants were calculated as a function of different Cu concentrations.

Results and Discussion

Figure (1) shows the X-ray diffraction patterns for pure and doped CdS films with different doping ratio with Cu (0,5 and 10%) this figure indicate all films have polycrystalline structure and have a good identically with standard peaks for both hexagonal and cubic CdS with increasing the hexagonal phase with increasing Cu ratio. In addition we can also see from table (1) a decreasing in d_{hkl} with increasing Cu content i.e., slightly shift in 2θ to higher value (as shown in the two dimensional intensity, figure 2) because the size of Cu ion (which have been inserted into lattice) less than for Cd ion.

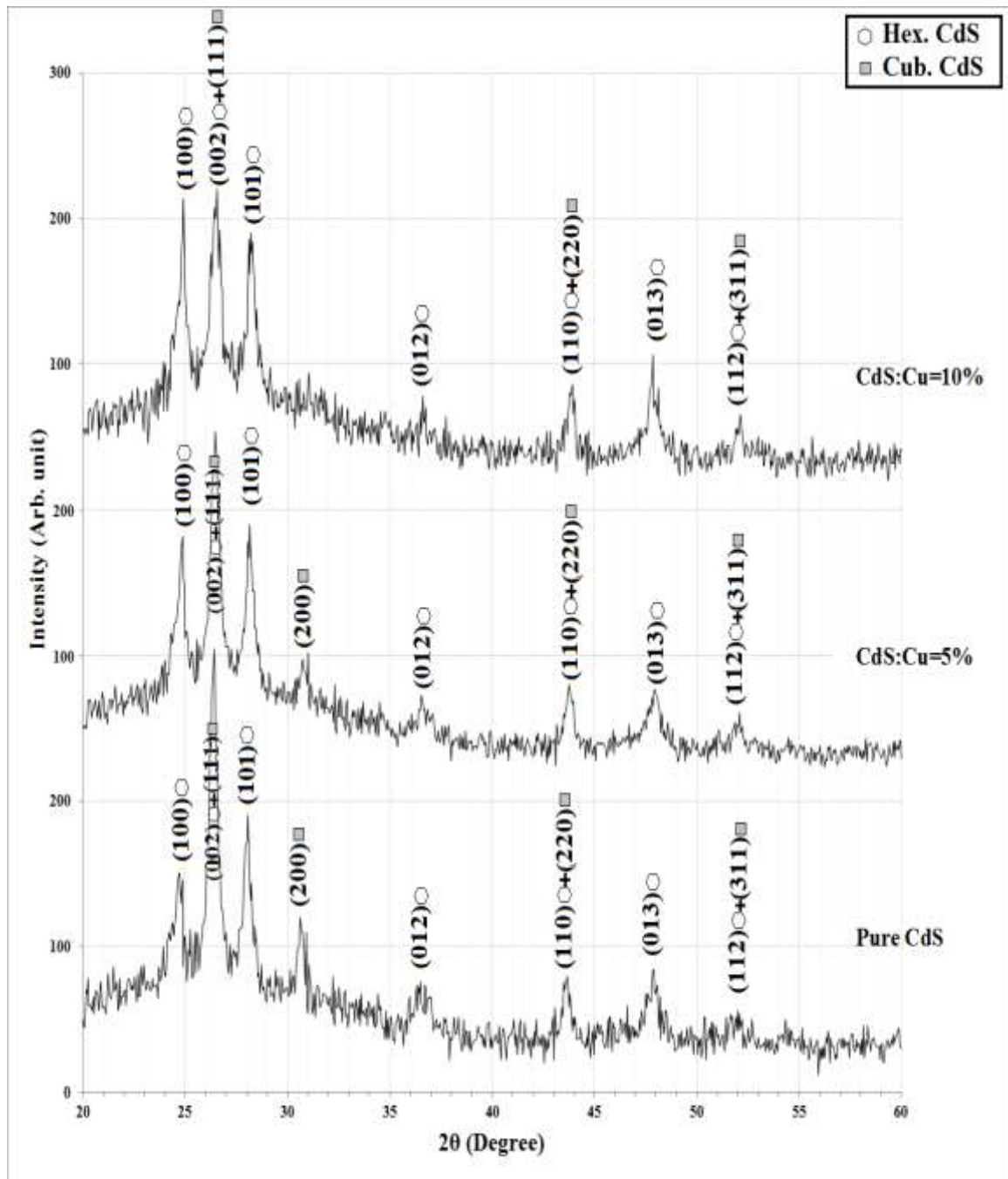
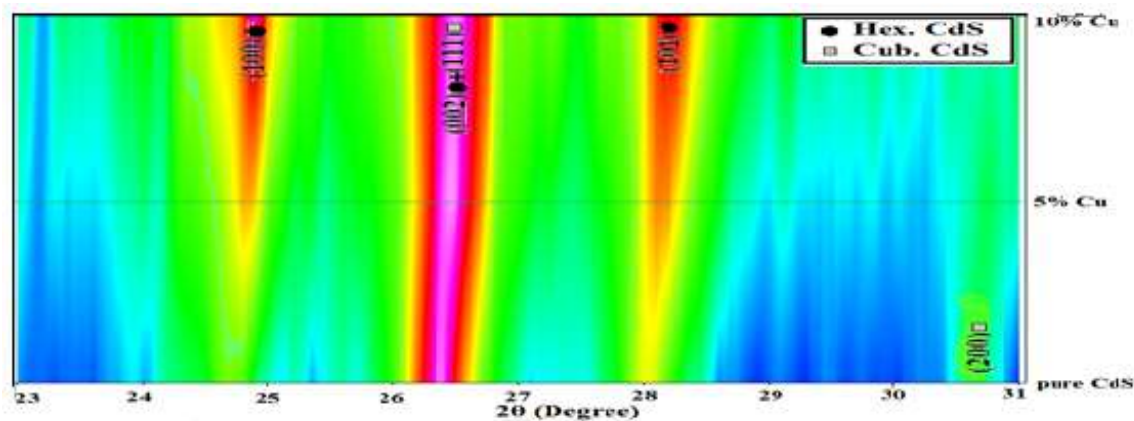


Fig. (1) X-ray diffraction patterns for Cd_{1-x}S Cu_x with different Cu ratio (0, 5 and 10%)

Table (1) Structural parameters: Inter-planar spacing, crystalline size of deposited pure and doped CdS films at different Cu doping ratio (0, 5 and 10) %.

Cu %	2θ (Deg.)	FWHM (Deg.)	d _{hkl} Exp.(Å)	G.S (nm)	d _{hkl} Std.(Å)	hkl	phase	card No.
0	24.7084	0.6872	3.6003	11.8	3.5827	(100)	Hex. CdS	96-901-1664
	26.4363	0.4754	3.3688	17.2	3.3572	(002)	Hex. CdS	96-901-1664
					3.3677	(111)	Cub. CdS	96-900-0109
	28.0778	0.4385	3.1754	18.7	3.1609	(101)	Hex. CdS	96-901-1664
	30.6263	0.5330	2.9168	15.5	2.9165	(200)	Cub. CdS	96-900-0109
	36.5011	1.2099	2.4597	6.9	2.4498	(012)	Hex. CdS	96-901-1664
	43.6717	0.7962	2.0710	10.7	2.0685	(110)	Hex. CdS	96-901-1664
					2.0623	(220)	Cub. CdS	96-900-0109
	47.8618	0.9942	1.8990	8.7	1.8982	(013)	Hex. CdS	96-901-1664
52.0086	0.9651	1.7569	9.2	1.7611	(112)	Hex. CdS	96-901-1664	
				1.7587	(311)	Cub. CdS	96-900-0109	
5	24.8812	0.3771	3.5757	21.6	3.5827	(100)	Hex. CdS	96-901-1664
	26.4795	0.5211	3.3634	15.7	3.3572	(002)	Hex. CdS	96-901-1664
					3.3677	(111)	Cub. CdS	96-900-0109
	28.1641	0.4002	3.1659	20.5	3.1609	(101)	Hex. CdS	96-901-1664
	30.7559	0.7722	2.9048	10.7	2.9165	(200)	Cub. CdS	96-900-0109
	36.5443	0.7930	2.4569	10.5	2.4498	(012)	Hex. CdS	96-901-1664
	43.7581	0.4863	2.0671	17.6	2.0685	(110)	Hex. CdS	96-901-1664
					2.0623	(220)	Cub. CdS	96-900-0109
	47.9482	0.7351	1.8958	11.8	1.8982	(013)	Hex. CdS	96-901-1664
52.0518	0.5313	1.7556	16.6	1.7611	(112)	Hex. CdS	96-901-1664	
				1.7587	(311)	Cub. CdS	96-900-0109	
10	24.9244	0.4191	3.5696	19.4	3.5827	(100)	Hex. CdS	96-901-1664
	26.5659	0.5911	3.3526	13.8	3.3572	(002)	Hex. CdS	96-901-1664
					3.3677	(111)	Cub. CdS	96-900-0109
	28.2073	0.4653	3.1611	17.6	3.1609	(101)	Hex. CdS	96-901-1664
	36.6307	0.2991	2.4513	28.0	2.4498	(012)	Hex. CdS	96-901-1664
	43.9309	0.4634	2.0594	18.5	2.0685	(110)	Hex. CdS	96-901-1664
					2.0623	(220)	Cub. CdS	96-900-0109
	47.9050	0.5687	1.8974	15.3	1.8982	(013)	Hex. CdS	96-901-1664
	52.1382	0.4815	1.7529	18.4	1.7611	(112)	Hex. CdS	96-901-1664
1.7587					(311)	Cub. CdS	96-900-0109	



Fig(2) Two dimensional X-ray diffraction patterns intensities for Cd_{1-x}S Cu_x with different Cu ratio (0, 5 and 10%)

Table (2) shows a decrement in lattice constants for Hexagonal and cubic phases which have been observed in XRD patterns

Table (2) Lattice constants for Hexagonal and cubic observed phases in XRD patterns

Cu: Cd%	Cubic	Hex	
	a (nm)	a(nm)	c (nm)
0	5.8349	4.1573	6.7376
5	5.8256	4.1289	6.7268
10	5.8069	4.1218	6.7052

Optical measurements for deposited $Cd_{1-x}S Cu_x$ films on glass substrate with different doping concentrations are carried out in the wavelength range 400–1100 nm at room temperature. Figure (3) shows the room temperature transmittance spectra for samples doped with different Cu concentrations. This figure shows that the transmittance increases with increasing of wavelength (λ). On the other hand the transmittance decreases with the increase of Cu concentration

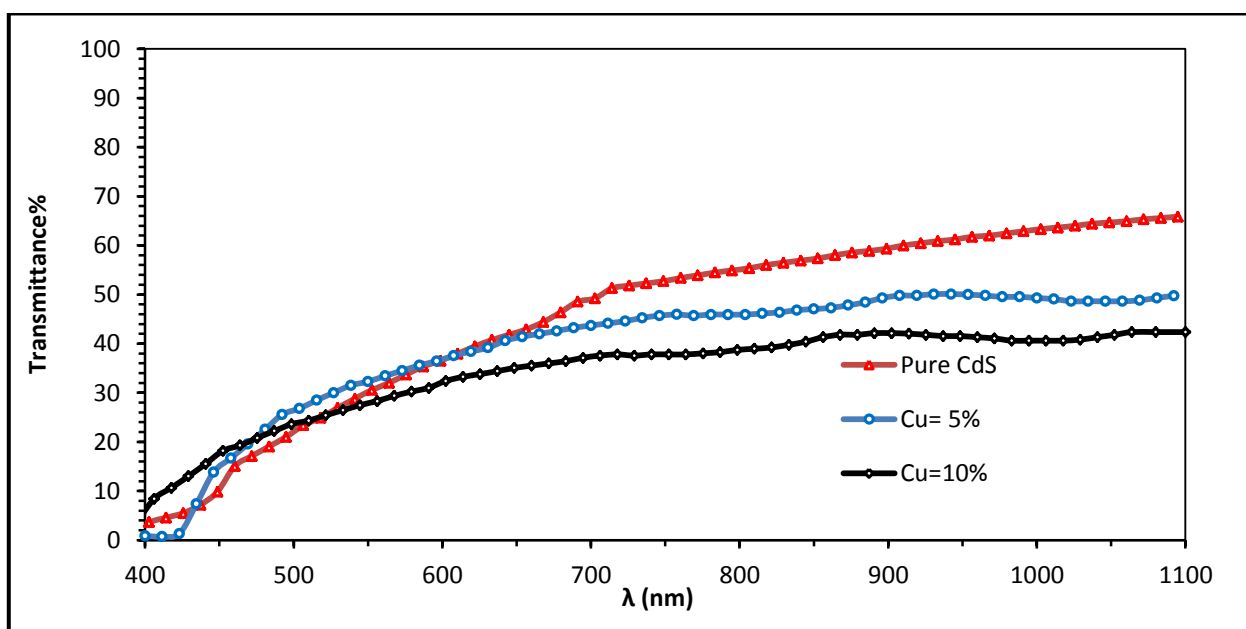


Fig.(3) Transmittance variation with the wavelength for pure and doped CdS films with Cu.

Figs.(4) illustrates the variation of absorption coefficient with wavelength for $Cd_{1-x}S Cu_x$ films on glass substrate with different doping concentrations. All spectra illustrate absorption coefficient pattern of all deposited pure and doped thin CdS films decrease with increasing of wavelength (λ) from 400 to 1100 nm. On the other hand the absorption coefficient increases with the increase of Cu concentration.

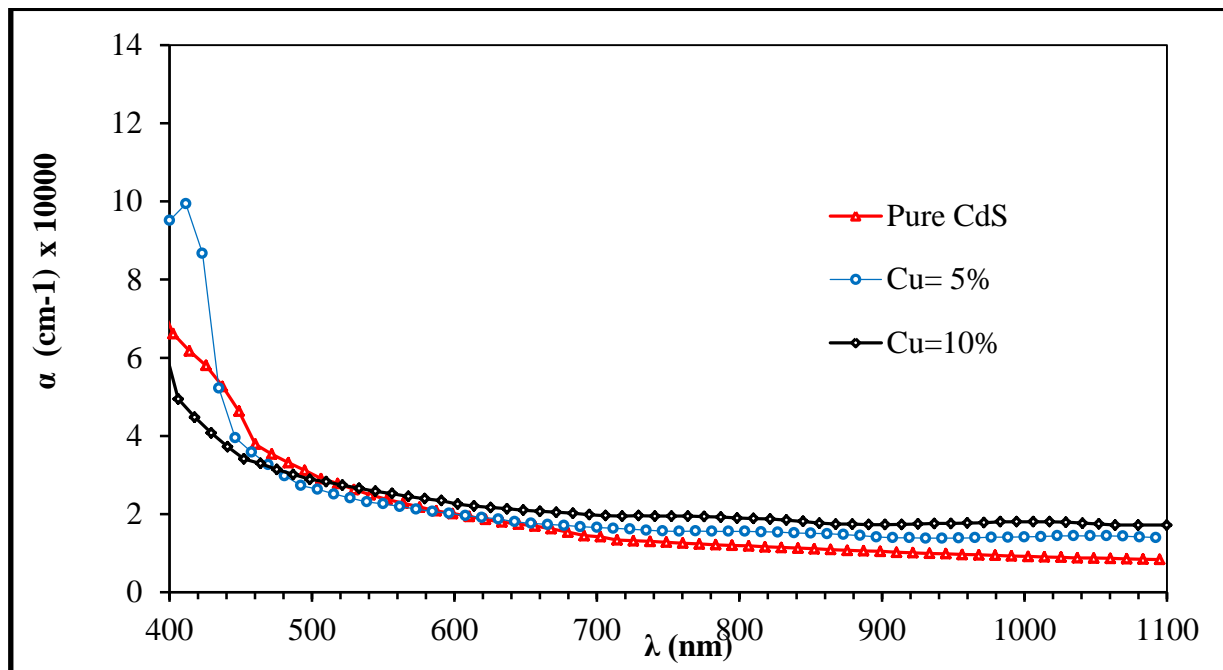


Fig.(4) Variation of absorbance coefficient with the wavelength for pure and doped CdS films with Cu.

The optical energy gap values (E_g^{opt}) for thin CdS films on glass have been determined by using Tauc equation^[8].

$$\alpha h\nu = A \left(h\nu - E_g \right)^r$$

where $h\nu$ is the photon energy, E_g is the optical band gap energy, A is inversely proportional to amorphousity and r is used to find the type of the optical transition by plotting the relations $(\alpha h\nu)^{1/2}$, $(\alpha h\nu)^{1/3}$, $(\alpha h\nu)^{2/3}$, and $(\alpha h\nu)^2$ versus photon energy ($h\nu$). The energy gap (E_g) is then determined by the extrapolation of the linear portion at $(\alpha h\nu)^2 = 0$. It is found that the relation for $r=1/2$ yields linear dependence part at which the absorption coefficient $\alpha \geq 10^4 \text{cm}^{-1}$, which describes that $\text{Cd}_{1-x}\text{SCu}_x$ films have the allowed direct transition. This result is in agreement with result had shown by the previous researches.

The variation of $(\alpha h\nu)^2$ as a function of photon energy for pure and Cu doped thin CdS films at different Cu concentration has been plotted in Fig.(5). This figure reveals that the increasing of Cu concentrations from 0 to 10% leads to increase the energy gap from approximately 2.34eV to 2.45eV. This can be attributed to decrease the lattice constants.^[9]

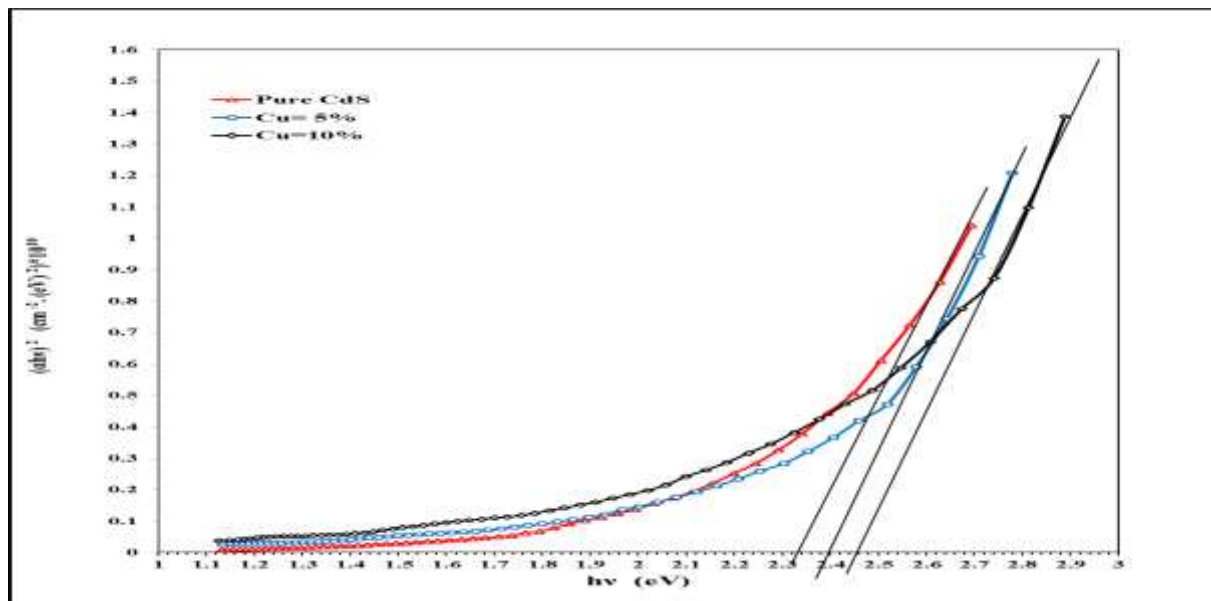


Fig.(5) The variation of $(\alpha hv)^2$ versus photon energy ($h\nu$) for for pure and doped CdS films with Cu.

It is important to determine the optical constants of thin films such as refractive index (n), extinction coefficient (k), and the real (ϵ_r) and imaginary (ϵ_i) parts of dielectric constant.

Fig.(6) shows the variation of extinction coefficient with wavelength at different Cu doping ratio. The extinction coefficient depends mainly on absorption coefficient; for this reason, the behavior of it is similar for absorption coefficient i.e., the increasing of extinction coefficient with increasing photon energy because the absorption is increased.

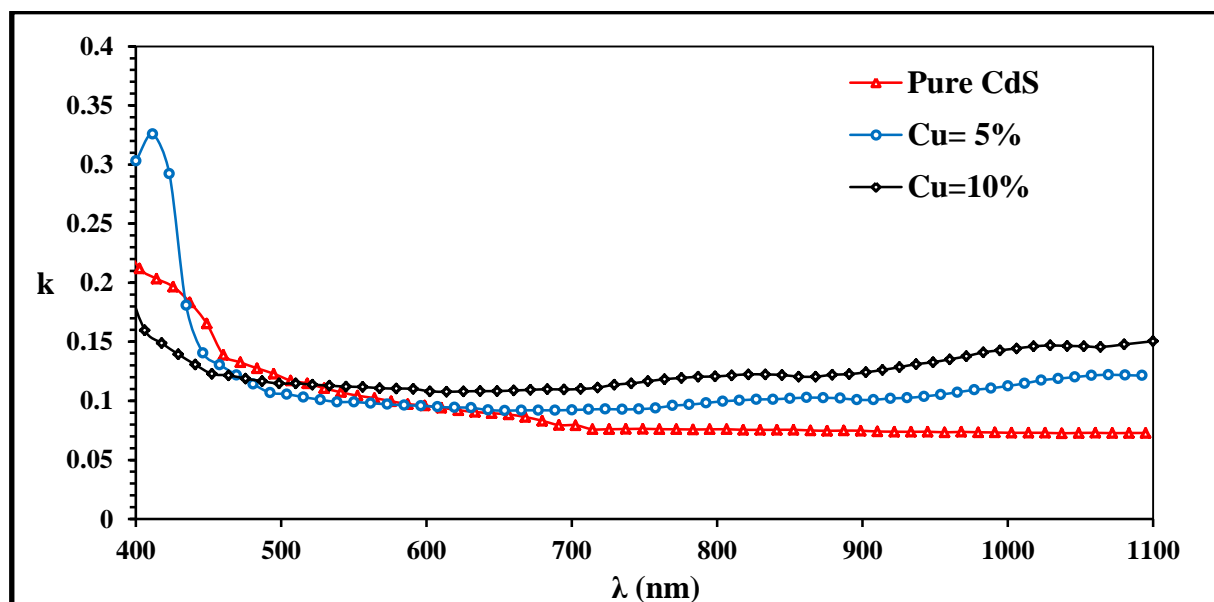


Fig. (6) Extinction coefficient versus wavelength for pure and doped CdS films with Cu.

The index of refraction of pure and Cu doped thin CdS films was estimated from the reflectance (R) data using the relation ^[10]:

$$n = \sqrt{\frac{4R}{(1-R)^2} - k^2} - \frac{R+1}{R-1}$$

The variation of the refractive index versus wavelength in the range 400–1100 nm, for deposited CdS films on glass with different Cu doping concentrations films have been shown in Fig. (7). It is clear from this figure that the refractive index in general increases with increasing of doping concentration with Cu.

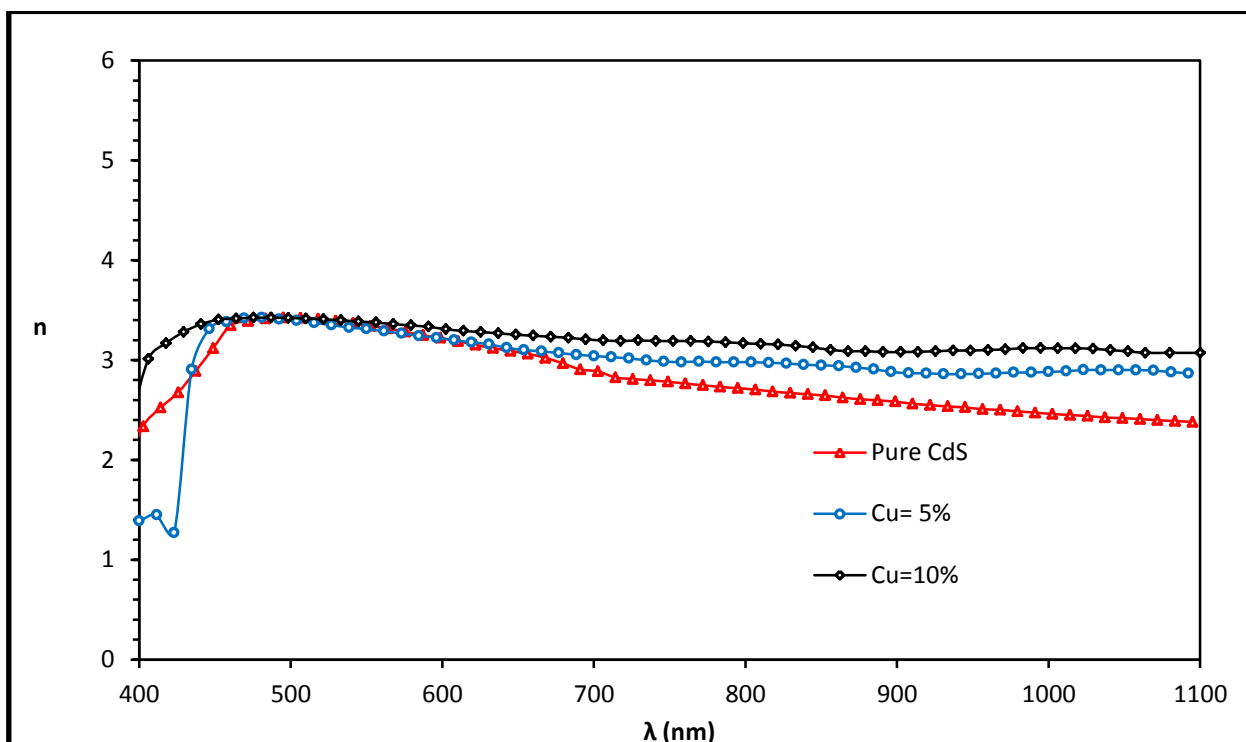


Fig. (7)The variation of refractive index with the wavelength for pure and doped CdS films with Cu.

The real and imaginary parts of dielectric constant were evaluated using the formulas ^[11]:

$$\epsilon_r = n^2 - k^2$$

$$\epsilon_i = 2nk$$

The variation of the real and imaginary parts of the dielectric constants values versus wavelength have been shown in figures (8 and 9) for deposited pure and Cu doped thin CdS films on glass with different doping concentrations. Their value are decreased with wavelength more than 500nm. The variation of the dielectric constant depends on the value of the refractive index. By contrast, the dielectric loss depends mainly on the extinction coefficient values which are related to the variation of absorption.

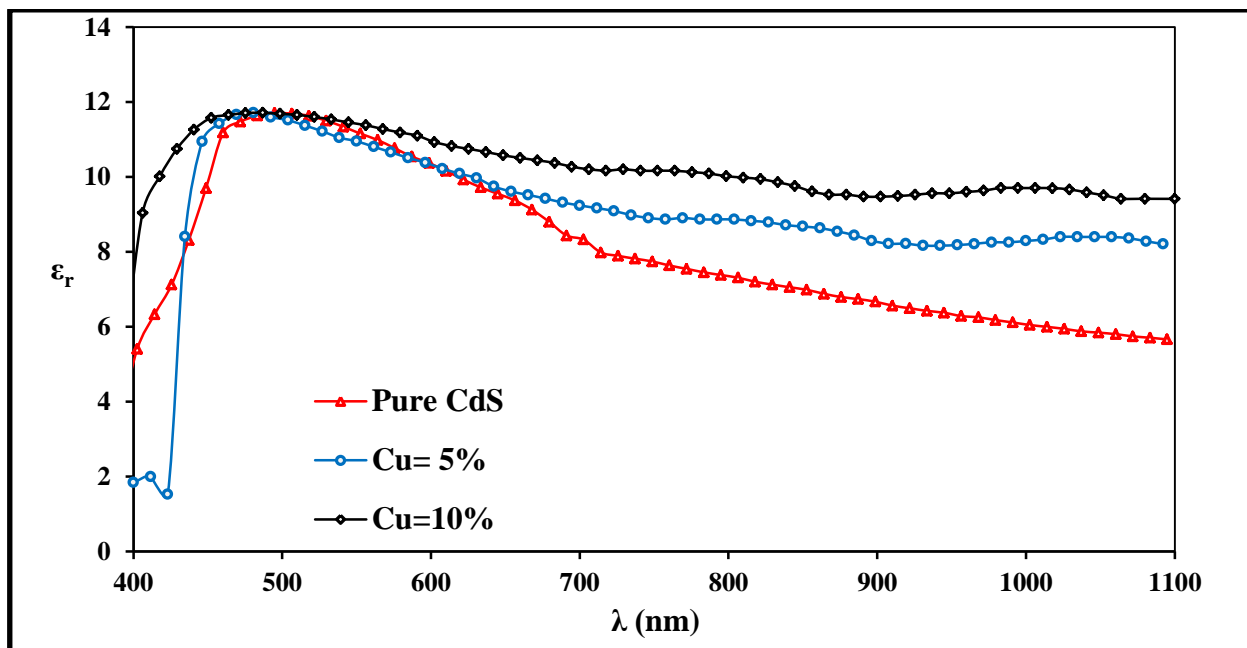


Fig.(8) The variation of ϵ_r with the wave length for pure and doped CdS films with Cu.

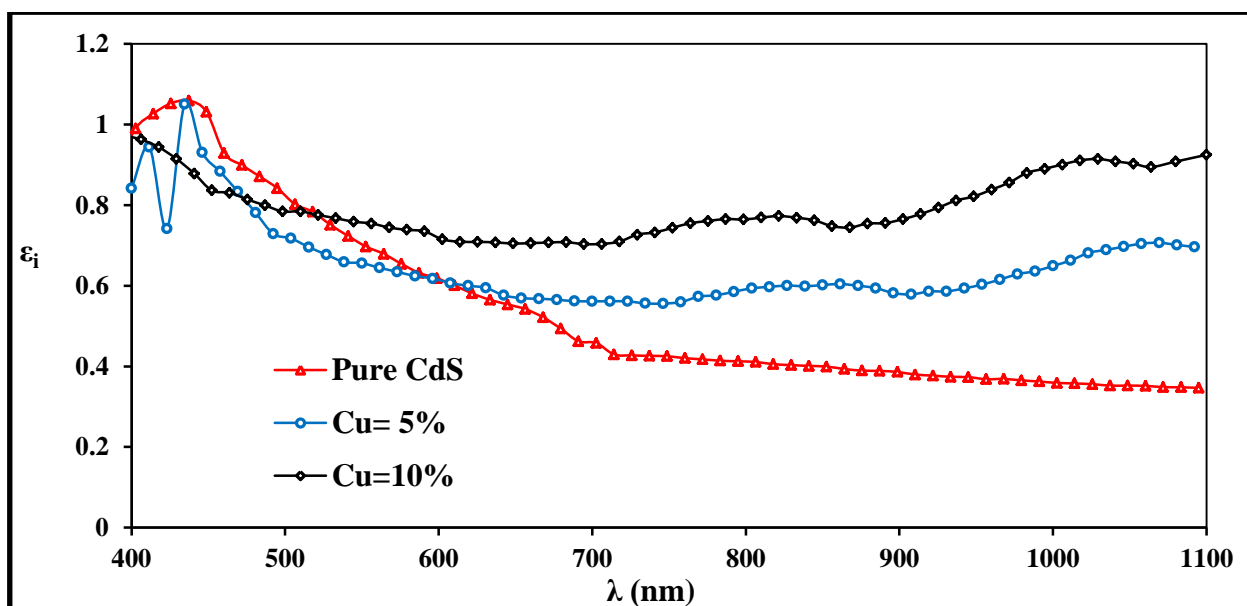


Fig.(9) The variation of ϵ_i with the wave length for pure and doped CdS films with Cu.

Table (1) shows the optical constants for deposited pure and Cu doped thin CdS films on glass with different doping concentrations (0, 5 and 10%) at $\lambda = 800$ nm and the optical gap values for these prepared samples. This Table illustrates that the values of α , k , n , ϵ_r , ϵ_i and E_g increase with increasing Cu dopant concentrations, whereas the behavior of T is opposite i.e., decrease with increasing Cu doping concentrations.

Table (1) The optical parameters at $\lambda=800$ nm and E_g for pure and doped CdS films at different Cu doping concentrations.

Cu%	T%	α (cm ⁻¹)	K	n	ϵ_r	ϵ_i	E_g (eV)
0	54.91	11992	0.076	2.718	7.381	0.413	2.34
5	45.92	15567	0.098	2.979	8.866	0.585	2.40
10	38.73	18976	0.121	3.168	10.021	0.764	2.45

Conclusions

Structural and optical properties of Cd_{1-x}SCu_x thin films deposited by spray pyrolysis deposition technique have been studied as a function of different Cu dopant concentrations. The outcome of this investigation can be summarized as follows:

- XRD indicates that all Cd_{1-x}SCu_x films have polycrystalline structure and have both hexagonal and cubic CdS phases and increasing the hexagonal phase with increasing Cu ratio.
- Decreasing in d_{hkl} with increasing Cu content i.e., slightly shift in 2θ to higher because the size of Cu ion less than for Cd ion. i.e decreasing in lattice constants.
- The transmittance increases with increasing wavelength while it decreases with increasing Cu doping concentrations.
- The energy gap increases from 2.34eV to 2.45eV with the increase of Cu doping concentrations from 0 to 10% due to the decrement in lattice constants.
- The optical constants values (α , k , n , ϵ_r and ϵ_i) increase with increasing Cu dopant concentrations,

References

- [1] S. Kar and S. Chaudhuri, *Met. Org. Nano-Metal Chem.* 36, (2006), p: 289–312.
- [2] Xu Y. N., Ching W. Y., "Electronic, optical, and structural properties of some wurtzite crystals", *Physical Review B*, 48, (1993), p: 4335-4351.
- [3] B. Skinner "Unit-cell edges of natural and synthetic sphalerites Locality: synthetic", *American Mineralogist*, 46, (1961), p:1399-1411.
- [4] J. Ximello-Quiebras, G. Contreras-Puente, J. Aguilar-Hernandez, G. Santana Rodriguez and A. Arias-Carbajal Readigos, *Sol. Energ. Mater. Sol Cells*, 82, (2004), p: 263.
- [5] *Fundamentals of the Physics of Solids, Vol. I Structure and Dynamics* Translated by Attila, (1999), Piroth, p: 242,261.
- [6] B. Warren, *X-ray Diffraction*, Addison-Wesley Publishing Company, (1969), p:253.
- [7] Z. Rizwan, A. Zakaria, M. Ghazali, A. Jafari, F. Ud Din, and R. Zamiri, *Int. J. Mol. Sci.*, 12, (2011), p: 1293.
- [8] J. Tauc, "Amorphous and Liquid Semiconductors", Plenum Press, London and New York (1974).
- [9] S. M. Sze and Kwok K. Ng "Physics of Semiconductor Devices "Third Edition, A John Wiley & Sons, Inc., Publication, (2006), p: 60.
- [10] S. Aksoy, Y. Caglar, S. Ilcan, and M. Caglar, *Optica Applicata*, V. XL, N.1 (2010), p: 7.
- [11] L. Kazmerski, "Polycrystalline and Amorphous Thin Films and Devices", Academic Press (1980).